Nonlinearity

Cover illustration: Polygonal hydraulic jumps

To cite this article: Clive Ellegaard *et al* 1999 *Nonlinearity* **12** 1

Nonlinearity **12** (1999) 1–7. Printed in the UK PII: S0951-7715(99)98777-7

Cover illustration: Polygonal hydraulic jumps

Clive Ellegaard, Adam Espe Hansen, Anders Haaning, Kim Hansen, Anders Marcussen, Tomas Bohr†‡, Jonas Lundbek Hansen§ and Shinya Watanabe‖

Center for Chaos and Turbulence Studies, The Niels Bohr Institute, Blegdamsvej 17, DK-2100, Copenhagen Ø, Denmark

Received 27 October 1998, in final form 12 November 1998

This year's cover illustration shows an unexpected singular structure occurring in a flow seen in an ordinary household kitchen sink. When a vertical jet of liquid impinges on a flat surface it creates a ring discontinuity, the *circular hydraulic jump*, at a well-defined distance from the jet, where the depth of the fluid layer changes by an order of magnitude. By using a liquid more viscous than water, we have noticed [1] that the circular hydraulic jump may spontaneously deform to a *polygonal* structure (as shown in figure 1) breaking the axial symmetry. The corners can be very sharp and carry a large radial flux while the edges (sides) generate resistance on the stream. We describe this experiment in detail, and present a heuristic explanation of the rather aesthetically pleasing states. The explanation is admittedly not systematic, but illuminates the role of the internal eddy structure in the flow, and qualitatively agrees with the observed parameter dependence.

The circular hydraulic jump is a familiar phenomenon, in which a flow experiences a strong surface deformation [2–11]. It is remarkable because it allows the observation of strongly nonlinear phenomena like shocks and wave breaking under laminar, stationary conditions. It is closely akin to flows occurring in channels, rivers, beaches and the atmosphere. Although these flows tend to have much larger spatial scales and thus be turbulent, the table-top circular jump geometry is expected to illuminate many important features of these flows.

Following a classic idea by Lord Rayleigh [2], we have designed an experiment as shown schematically in figure 2(a). Close to the jet, the fluid layer is thin (height h_{in}) and the motion is rapid, whereas further away, the layer height has increased by an order of magnitude to h_{ext}, and the fluid moves correspondingly more slowly. The transition between these two types of motion occurs within a surprisingly short distance: a millimeter or so. The horizontal surface is a disc of a large diameter (36 cm), made of glass so that the jump can be observed from below. The rim around the disc can be raised or lowered in order to control h_{ext}. (Note that even when the rim height is zero, a jump still occurs. Raising the rim forces the jump to be stronger.) The fluid going over the rim is collected and recirculated; the flow rate Q from the jet is kept constant. The flow patterns are visualized using fine aluminium powders. It is a simple experiment, but particular care is needed to secure smoothness of the horizontal surface and the nozzle, which also needs to be long enough to avoid disturbances. We have described

† Correspondence and requests for materials: tbohr@nbi.dk
‡ Present address: Physics Institute, Building 309, The Danish Technical University, DK-2800 Lyngby, Denmark.
§ Present address: Danish Defence Research Establishment, Ryvangs Allé 1, Postboks 2715, DK 2100 Ø, Denmark.
‖ Present address: Mathematical Sciences Department, Ibaraki University, Mito 310-8512, Japan.

0951-7715/99/010001+07$19.50

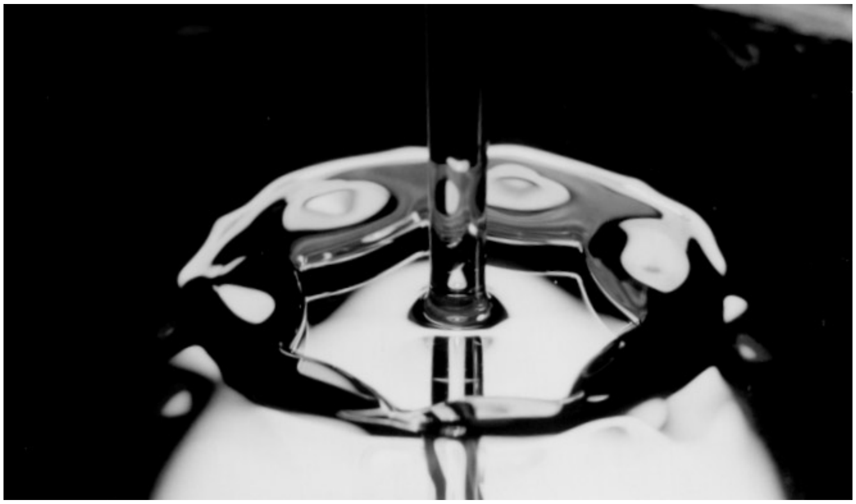

Figure 1. The polygonal hydraulic jump is an intriguing stationary flow that occurs on a table top. Here, a heptagonal case is shown. The distance of the jump from the impinging jet is about 2 cm.

the experimental details elsewhere [10].

The circular jump shows two states, with different cross-sectional flow patterns [10]. When h_{ext} is small, we observe a 'type I' pattern in which the surface velocity is outward everywhere and a separation bubble is present at the bottom right outside the jump. On increasing h_{ext} the jump becomes steeper until, at a critical h_{ext}, fluid outside the jump topples over and breaks. When a new steady state ('type II' pattern) is reached, a surface eddy has formed. This eddy, called a 'roller' or a 'surfing wave,' has the geometry of a floating torus surrounding the jump (figure 2(a)). The outgoing flow passes under the roller. This maintains the rotation of the roller and an inward surface velocity near the jump.

Water was used in the initial experiments, but the flow, especially type II, was rather unstable and nonstationary. Viscous ethylene glycol (antifreeze) was added, with the aim of producing a 'clean' circular type II state. Unexpectedly, however, this state frequently undergoes spontaneous breaking of the azimuthal symmetry into a stationary *polygonal* shape. Rather than weak angular deformations which one would generally expect in fluids, the jumps form clear corners with edges that are often straight, as seen in figure 2(c) and (d). As h_{ext} is raised from the type I regime, the transition to the type II regime may render the circular jump unstable, so that it will deform to a polygon with a large number of corners. Polygons with up to 14 corners are observed by changing the flow rate Q, the height of the nozzle outlet h_{noz}, and the kinematic viscosity ν. As h_{ext} is increased further, corners disappear, usually one by one, and the circumference of the jump becomes smaller until the jump eventually 'closes.' The phase diagram is shown in figure 3, varying h_{ext}, h_{noz} and Q. Four jumps visualized from directly below are shown in figure 4.

How can such singular flow structures occur in these simple flows? The systematic approach to such a problem would be to view the phenomenon as an instability of the circular hydraulic jump, and identify the unstable modes. This approach is possible, for example in [12], corners were observed during the breaking of a spinning drop. In that example, the basic flows are slow and can be handled within the lubrication approximation. The basic state can be found in the simplified set of equations. In our case, however, the Reynolds number is of moderate size, estimated to be 20–300 using the film thickness and the average velocity just

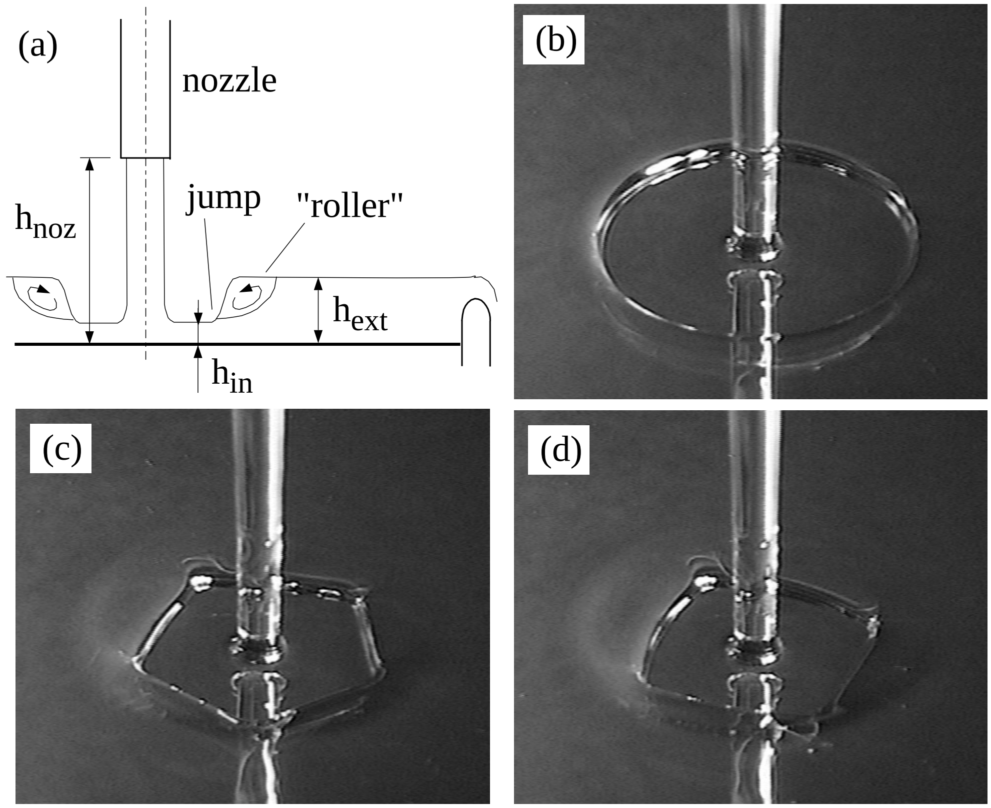

Figure 2. Schematic drawing of the hydraulic jump experiment and a cross-sectional flow structure (‘type II’ pattern) is shown in (a), while (b)–(d) show video images of three stationary states. The fluid is ethylene glycol (antifreeze, around 99% pure). The external height h_{ext} is increased from (b) to (d). The familiar circular jump in (b) changes spontaneously to a polygonal shape, for example, a pentagon (c), or a square (d). These states are robust; they reappear if the flow is temporarily disrupted or scrambled. However, several polygon states can be stable for the same h_{ext}, and additional corners can be created by locally dragging a side of the jump using a pin. Corners prefer to be equally spaced; if not, an adjustment in the azimuthal direction occurs over a long time (sometimes hours).

inside the jump. In this case, simplification of the Navier–Stokes equations with either large or small Reynolds number is not applicable. In addition the basic state, the circular type II flow, has a strongly deformed surface, and hence is not known well enough, not even numerically, to carry out the stability analysis. Therefore, the following heuristic model is of value in order to identify relevant parameters and to explain qualitatively the mechanism.

Since we observe polygons only in the type II flows, the explanation must be sought in the presence of the roller outside the jump. Recall that the stream from the jet has to penetrate through the narrow zone under the roller, thus experiencing a resistance force. The wider the roller, the harder it is to flow out. Thus, a portion of mass flux, initially injected uniformly by the jet, is redirected from wider parts (i.e. edges of the polygons) to narrower parts (corners). This picture is supported by the observation of rapid radial jets shooting out at the corners while the flow is calmer outside the edges.

Let us make the picture more quantitative. The fluid height is h_{in} inside the jump, and h_{ext} outside. The radial flux q depends on the azimuthal angle θ, and must add up to the total

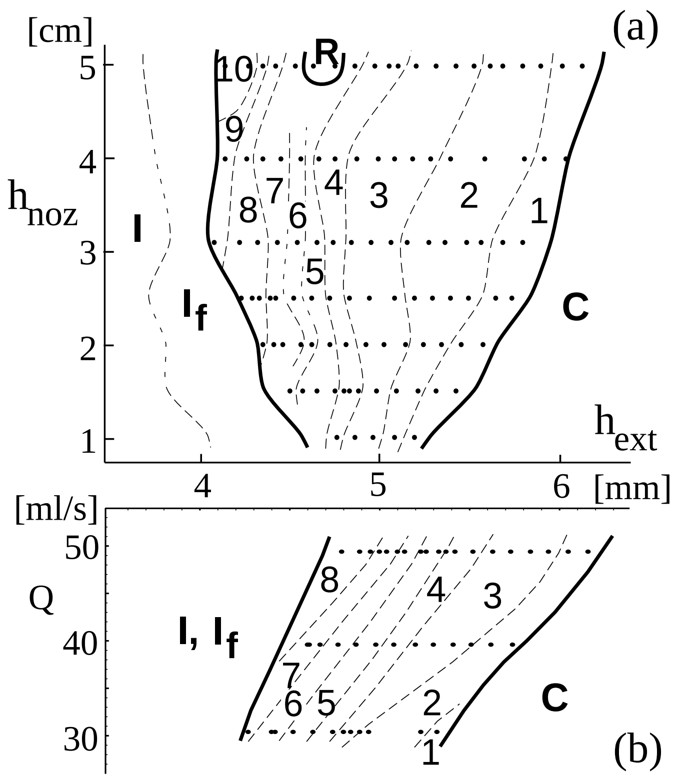

Figure 3. The phase diagram of the stable states. The external fluid height h_{ext} and the nozzle height h_{noz} is changed in (a) while the flow rate Q and h_{ext} are varied in (b). The fixed parameters are Q ($\approx$40 ml s^{-1}) and the kinematic viscosity ν ($\approx$10 times that of water) in (a), and h_{noz} ($= 2$ cm) and ν ($\approx$11 times water) in (b). In both panels the actual measurements are marked as dots. For small h_{ext} the circular 'type I' jump (labelled **I**) is observed. Increasing h_{ext}, the jump is still circular and stable, but small surface fluctuations are superimposed in the region $\mathbf{I_f}$. For large enough h_{ext} the radius of the jump becomes very small and then disappears in the region **C**. Between $\mathbf{I_f}$ and **C**, polygons of various numbers of corners are observed as shown. Several polygons can be stable for the same parameters. We have disturbed the flow a number of times and determined the most likely number of corners at each marked point. Most patterns are completely stationary, but $\mathbf{I_f}$, **C**, and sometimes polygons with a small number of corners fluctuate in time. The region marked as **R** in (a) is qualitatively different. Polygons are not stable here, and the corners disappear very slowly (taking more than an hour) finally leaving a round type II state. As h_{noz} is increased beyond 5 cm, this region becomes wider, and stable polygons become harder to find. In (a) the dependence of h_{noz} on the number of corners is weak, as the boundary curves of 4–8 corners are roughly vertical. In (b) the boundary curves show stronger dependence on Q. These features are in qualitative agreement with our heuristic model.

flux $Q = \int_0^{2\pi} q(\theta)\mathrm{d}\theta$. To describe how q depends on the width $y(\theta)$ of the roller, consider radial forces acting on the roller. The roller is subject to shear from the main flow in the outward direction; an estimate of the force is proportional to $\rho\nu q y/h_j^2$ where ρ is the density, and $h_j = (h_{\mathrm{in}} + h_{\mathrm{ext}})/2$ is the mean thickness at the jump. The roller is also pushed inward because the fluid height is much larger outside the jump. This pressure force (assumed to be hydrostatic) is estimated to be $\rho g(h_{\mathrm{ext}} - h_{\mathrm{in}})^2/2$, where g is the gravitational acceleration. The shear and pressure forces point in the opposite directions and should be balanced. This balancing results in a simple relation, $q(\theta) \propto 1/y(\theta)$, which agrees with the above picture.

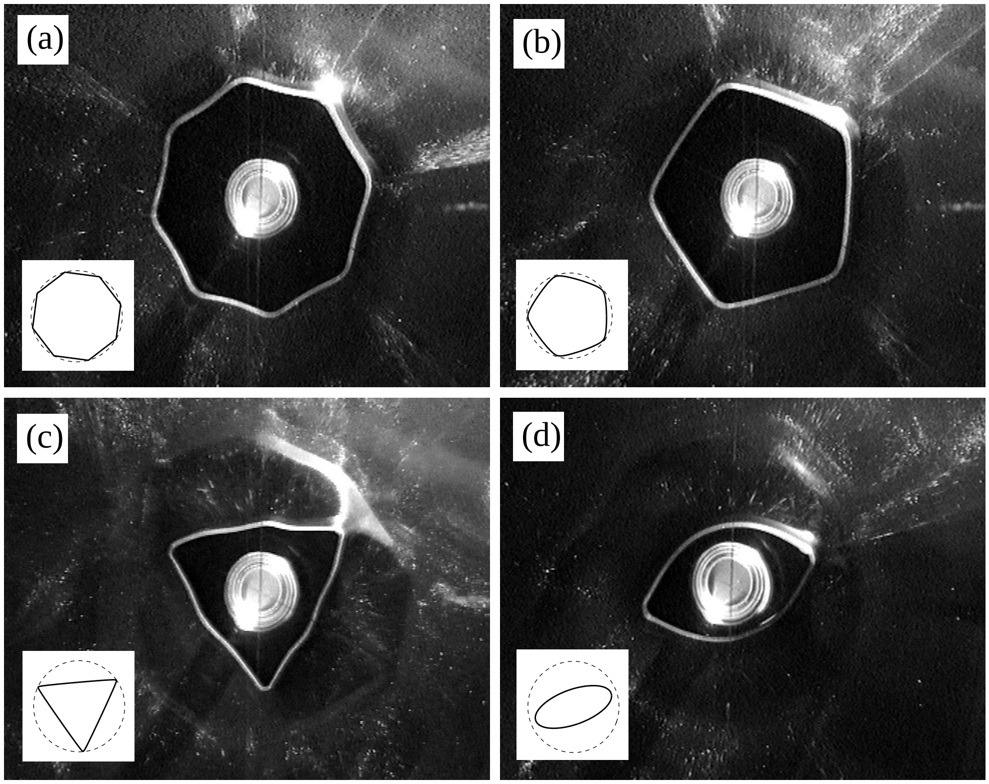

Figure 4. Polygon states with 8, 5, 3 and 2 corners (or radial jets), respectively, viewed from directly below through the horizontal glass plate. A bright circle in the centre is the vertical jet hitting the plate. The surrounding polygonal jump also appears bright, and shows clear corners; the sides are very curved in the 2-corner state. Solutions of our model are also shown in the insets. They are smooth functions which change rapidly at 'corners.'

There are still many $y(\theta)$ which satisfy the balance relation. One more criterion is necessary to select a particular shape. In experiments, when an edge of a polygon is perturbed slightly, its shape relaxes back by damped oscillations, as if it is an elastic string. Thus, it is natural to assume a weak line tension, such that the jump slowly evolves toward a stationary shape, with minimal circumference. The model is then well-posed as a minimization problem. The constraint imposed by the magnitude of the total flux Q can be handled by a Lagrange multiplier in the Euler–Lagrange equations for the stationary solutions. Formally, the problem reduces to the dynamics of a single particle in a potential, and it is possible to find the solutions and bifurcations in this model [13]. Four 'polygonal' solutions obtained in this way are shown in the insets of figure 4. Note that the function y is assumed to be smooth, but changes rapidly at evenly displaced θ. These locations can be considered as 'corners' (figure 4).

The model can be non-dimensionalized so that the sole parameter is the dimensionless flux:

$$\phi = \nu Q / \big(g\big(h_{\mathrm{ext}}^2 - h_{\mathrm{in}}^2\big)^2\big).$$

The circular jump exists for all ϕ, and this is the only solution for small ϕ. A polygonal jump with a given number of corners can be found only at an interval of ϕ; more corners are obtained as ϕ becomes larger. The intervals overlap so that several polygons can be solutions

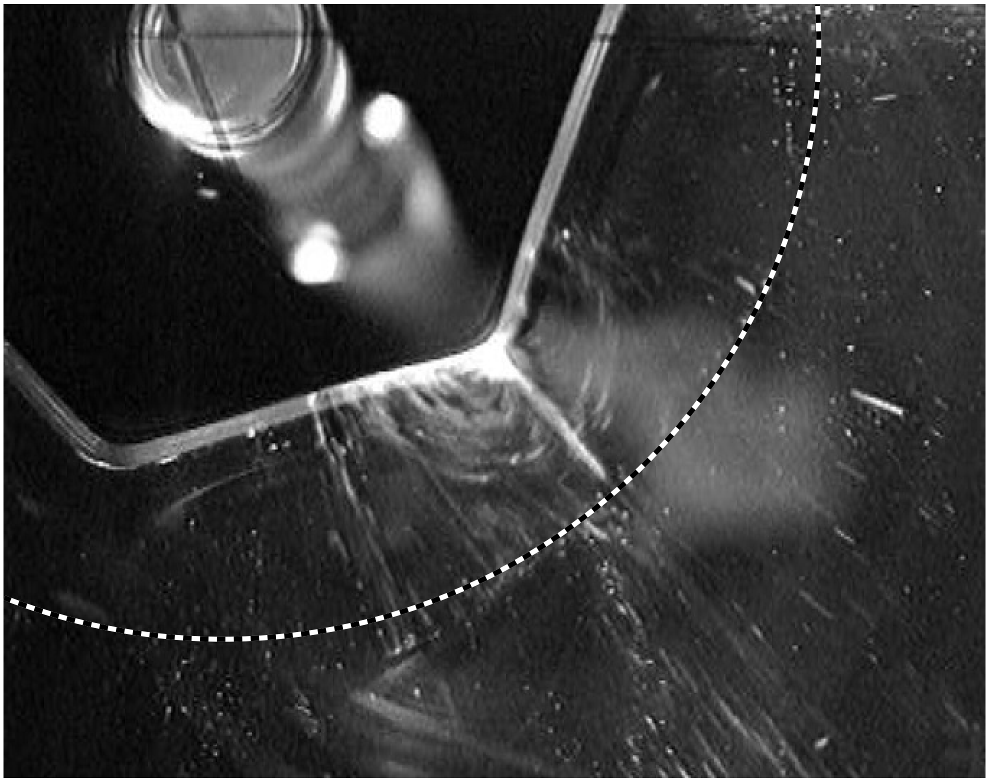

Figure 5. A close-up of a hexagonal state. The dotted line marks the inner edge of the separation zone on the bottom. The roller at the surface is situated within the region between the jump (bright straight line segments) and the dotted line. The main stream passes under the roller, and introduces internal flow in the roller. The streamlines visualized with aluminium powder indicate a complex three-dimensional structure near the corner and a break-up of the roller.

for the same ϕ, coinciding with the observed hysteresis. Several other experimental facts on the parameter dependence can be interpreted in the model. (i) When ν is small, e.g. water, we do not see stable polygons because ϕ is small. (ii) As $h_{\rm ext}$ is increased, ϕ decreases, giving fewer corners. (iii) Since $h_{\rm in}$ is less than one tenth of $h_{\rm ext}$ in the experiment, the dimensionless number ϕ is approximately $\phi \approx \nu Q/(g h_{\rm ext}^4)$. Thus, there is a strong dependence on Q and $h_{\rm ext}$ (see figure 3(b)), whereas the dependence on the nozzle height $h_{\rm noz}$, which affects only $h_{\rm in}$, is predicted to be weak in agreement with figure 3(a).

In our heuristic model we have assumed that the roller is a continuously deformable tube, but truly singular flows are typically observed near the corners. Figure 5 shows a close-up of a corner in a hexagonal type II state. The flow is rather complicated, with a secondary eddy visible on the surface, and it appears to us that the roller is actually ‘broken’ near the corner such that the free ends terminate at the fluid surface and create a large outward flux. Precisely at the corner the surface flow is thus outward like in the type I state. Along the edges inside the roller, we observe slow spiralling flow toward the corners. These observations suggest true three-dimensionality of the flow after the loss of the radial symmetry. Just as in an eccentric Taylor vortex flow [14], mixing between the roller and the main flow has become possible by the flow field forming chaotic streamline topology. More interestingly, the corner shape appears to be universal for given system parameters. We have set $h_{\rm ext}$ in a hysteretic regime, and scanned several polygons viewed from below. The angles and the shapes near the corners appear to overlap, irrespective of the number of edges. This forces the edges of the polygons to bend slightly inward (outward) for a large (small) numbers of corners.

Acknowledgments

We thank Vachtang Putkaradze, Martin van Hecke, Ken Haste Andersen and Hiraku Nishimori for many discussions in our group meetings. We also thank Stefan Mayer for important suggestions. SW appreciates hospitality from the IMA, University of Minnesota.

References

[1] Ellegaard C, Hansen A E, Haaning A, Hansen K, Marcussen A, Bohr T, Lundbek Hansen J and Watanabe S 1998 Creating corners in kitchen sinks *Nature* **392** 767
[2] Lord Rayleigh 1914 On the theory of long waves and bores *Proc. Roy. Soc.* A **90** 324
[3] Tani I 1949 Water jump in the boundary layer *J. Phys. Soc. Japan* **4** 212
[4] Watson E 1964 The radial spread of a liquid jet over a horizontal plane *J. Fluid Mech.* **20** 481
[5] Olsson R G and Turkdogan E T 1966 Radial spread of a liquid stream on a horizontal plate *Nature* **211**
[6] Craik A, Latham R, Fawkes R and Gribbon P 1981 The circular hydraulic jump *J. Fluid Mech.* **112** 347
[7] Bowles R and Smith F 1992 The standing hydraulic jump: theory, computations and comparisons with experiments *J. Fluid Mech.* **242** 145
[8] Bohr T, Dimon P and Putkaradze V 1993 Shallow-water approach to the circular hydraulic jump *J. Fluid Mech.* **254** 635
[9] Higuera F 1994 The hydraulic jump in a viscous laminar flow *J. Fluid Mech.* **274** 69
[10] Ellegaard C, Hansen A E, Haaning A and Bohr T 1996 Experimental results on flow separation and transitions in the circular hydraulic jump *Phys. Scr.* T **67** 105
Bohr T, Ellegaard C, Hansen A E and Haaning A 1996 Hydraulic jumps, flow separation and wave breaking: an experimental study *Physica* B **228** 1
[11] Bohr T, Putkaradze V and Watanabe S 1997 Averaging theory for the structure of hydraulic jumps and separation in laminar free surface flows *Phys. Rev. Lett.* **79** 1038
[12] Melo F, Joanny J F and Fauve S 1989 Fingering instability of spinning drops *Phys. Rev. Lett.* **63** 1958
[13] Watanabe S, Bohr T, Ellegaard C, Haaning A, Hansen A E, Hansen K, Lundbek Hansen J and Marcussen A unpublished
[14] Ashwin P and King G P 1995 Streamline topology in eccentric Taylor vortex flow *J. Fluid Mech.* **285** 215